Visible Optical Properties of Pulse-Laser-Melted Silicon with S, Se, Te, B, P and As

Si Hui Athena Pan

Martin A. Fisher School of Physics, Brandeis University

NNIN REU Site: Center for Nanoscale Systems, Harvard University, Cambridge, MA

NNIN REU Principal Investigator(s): Michael Aziz, School of Engineering and Applied Sciences, Harvard University

NNIN REU Mentor(s): Daniel Recht, School of Engineering and Applied Sciences, Harvard University

Contact: fromaspan@gmail.com, aziz@seas.harvard.edu, drecht@fas.harvard.edu

Introduction:

Recent research has demonstrated that laser-structured chalcogen-laden silicon (Si) exhibits enhanced electro-optical properties when compared with ordinary Si [1-3]. On the other hand, unstructured Si is more desirable for a wide variety of device architectures. Ion implantation followed by pulsed-laser-melting-induced rapid solidification provides a method to fabricate chalcogen-laden Si with a smooth surface and crystalline interior structure [4,5]. Sulfur-laden Si, fabricated through ion implantation and pulsed-laser-melting, has been shown to absorb light strongly in the near infrared region [5]. Until this work, the properties of laser-melted, chalcogen-laden Si in the visible spectrum have not been characterized. Furthermore, little has been done to compare these materials with Si supersaturated with common dopants such as boron. Here we present the preliminary results on the visible optical properties of pulse-laser-melted Si implanted with sulfur, selenium, tellurium, boron, arsenic and phosphorus (S, Se, Te, B, As and P, respectively).

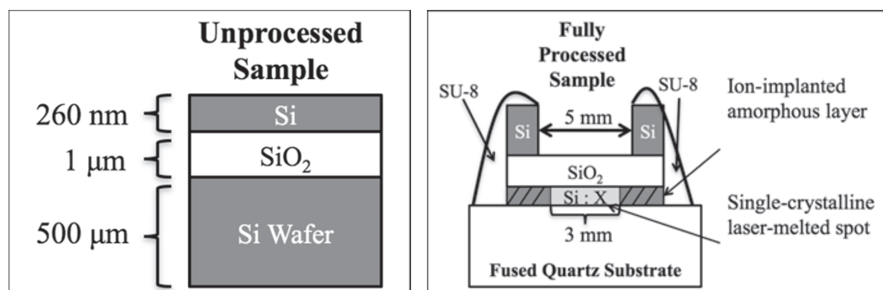

Figure 1, left: The schematic of the original SOI wafer.
Figure 2, right: The schematic of a completed processed sample.

Experimental Techniques:

Silicon on insulator (SOI) with dimensions shown in Figure 1 was used in this experiment. The 260 nm layer of p-Si(100) was ion implanted at room temperature with either $^{32}S^+$ at 80 keV, $^{80}Se^+$ at 125 keV, $^{130}Te^+$ at 120 keV, $^{11}B^+$ at 35 keV, $^{75}As^+$ at 110 keV or $^{31}P^+$ at 65 keV. Samples to be implanted at 1×10^{14} and 1×10^{15} S^+/cm^2 were first implanted with 3×10^{15} atom/cm^2 Si at 70 keV to produce a uniform amorphous layer.

The implantation dose ranged from 1×10^{14} to 3×10^{16} ions/cm^2. The ion-implanted samples were melted via irradiation with a pulsed $XeCl^+$ excimer laser (308 nm, 25 ns FWHM and 50 ns total duration) with a spatially homogenized beam. The laser fluence was controlled to be around 0.6~0.7 J/cm^2, which was chosen to melt to a depth between 210 and 250 nm. Time-resolved reflectivity of a low-power Ar^+ ion laser (488 nm) was used to monitor the melt duration [6].

After melting, the molten layer re-solidifies as a single crystal within a few nanoseconds so that a large amount of impurity atoms remain trapped within the alloy. The concentrations of implanted impurities were typically 2~4 orders of magnitude higher than equilibrium solubility [7]. Electron backscattering diffraction on a scanning electron microscope was conducted to confirm the single-crystal nature of the laser-melted layer of each sample.

In order to measure the visible optical properties of the ion-implanted layer, the bottom layer of plain Si (500 μm thick) must be removed. We polished this layer down to roughly 200 μm. The polished sample was then mounted onto a fused quartz substrate with SU-8 photoresist. The rest of the plain Si layer was removed by inductively-coupled plasma reactive ion etching. The schematic of a fully processed sample is shown in Figure 2.

We measured the transmittance of each sample with a Hitachi U-4001 spectrophotometer. A reflectance free method from Swanepoel was adopted to calculate the optical constants from transmittance only [8]. This method exploits the dependency of thin film interference fringes on the real (n) and imaginary (k) refractive indices. Such dependency allows the determination of n, k and the absorption coefficient α ($\alpha = 4\pi k/\lambda$), by simply interpolating smooth curves along the maxima and the minima of the fringes [8].

Results and Discussion:

Table 1 shows the real refractive indices n and the absorption coefficients α at 700 nm of samples implanted with different elements to different doses. All implanted samples have

refractive indices smaller than ordinary Si. The α of a low dose (1×10^{15} ions/cm^2) sulfur-implanted sample exhibits little difference from ordinary Si. However, the α of a high dose (1×10^{16} ions/cm^2) sulfur-implanted sample is increased by approximately 400% compared to ordinary Si at 700 nm. Figure 3 illustrates the α(λ) curves of both pure Si [9] and S-implanted Si at 1×10^{16} ions/cm^2 from 500 nm to 1.2 μm, which again shows the significant in-crease in absorption coefficient of the S-implanted sample.

Similarly, low dose selenium-implanted samples (1×10^{14} and 1×10^{15} ions/cm^2) exhibit only a small increase in the α compared to ordinary Si, while the difference in the α becomes more significant for high implantation doses. In particular, the absorption coefficient increases with the implantation dose. For the 3×10^{16} ion/cm^2 Se-implanted sample, α is an order of magnitude higher than that of ordinary Si.

Only high dose (1×10^{16} ion/cm^2) samples were processed and measured for Si supersaturated with Te, P, As and B. As shown in Table 1, high dose Te-implanted Si also possesses a much higher α than ordinary Si. Samples implanted with P, As and B also exhibit some increase in the α. However, such increase is relatively small compared to the three chalcogen elements investigated.

Comparing only the samples with an implantation dose of 1×10^{16} ion/cm^2, Se-implanted Si exhibits highest absorption among all elements, which is followed by S-implanted Si and Te-implanted Si. These preliminary results demonstrate chalcogen-laden Si absorbs visible light much more strongly than ordinary Si. The absorption mechanism is unknown, but hypotheses exist about the formation of an impurity band and about the formation of dopant nano-clusters. Potential applications of these strong-light-absorbing materials include the fabrication of low-cost photodetectors and photovoltaics since a thinner (and thus cheaper) layer could absorb all of the relevant light. Opto-electronic conversion for photodetectors has been demonstrated for laser-structured chalcogen-laden Si, but not yet in other settings.

Acknowledgements:

I would like to offer sincere thanks to my mentor, Daniel Recht, my P. I., Michael Aziz, and the rest of the Aziz group for their guidance and support, to the NNIN REU Program for providing me with this opportunity and to the NSF for funding this project.

References:

[1] C. Wu, C. H. Crouch, L. Zhao, J. E. Carey, R. Younkin, J. A. Levinson, E. Mazur, R.M. Farrell, P. Gothoskar, and A. Karger, Appl. Phs. Lett. 78, 1850 (2001).

[2] C. H. Crouch, J. E. Carey, J. M. Warrender, E. Mazur, M. J. Aziz, and F. Genin, Appl. Phys. Lett. 84, 1850 (2004).

[3] J. E. Carey, C. H. Crouch, M. A. Sheehy, M. Shen, C. M. Friend, and E. Mazur, Opt.Lett. 30, 1773 (2005).

[4] M. Tabbal, T. Kim, J. M. Warrender, M. J. Aziz, B. L. Cardozo, R. S. Goldman, J.Vac. Sci. Technol. B 25(6), 1847 (2007).

[5] T. G. Kim, J. M. Warrender, M. J. Aziz, Appl. Phys. Lett., 88, 241902 (2006).

[6] R. Reitano, P. M. Smith, and M. J. Aziz, J. Appl. Phys. 76, 1518 (1994).

[7] R. G. Wilson, J. Appl. Phys. 55, 3490 (1984).

[8] R. Swanepoel, J. Phys. E: Sci. Instrum. 16, 1214 (1983).

[9] R. Hull, Properties of crystalline silicon (IET, London, UK, 1999).

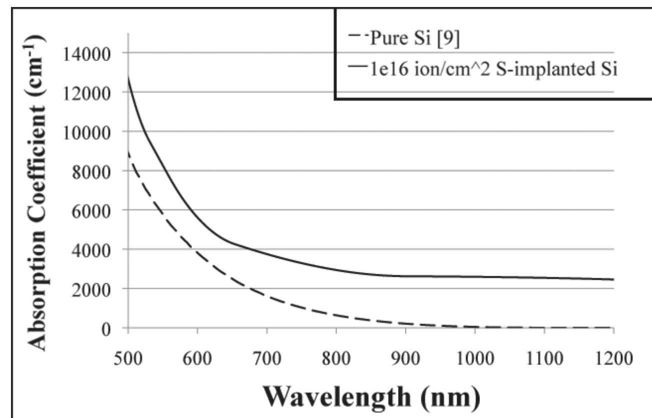

Figure 3, above: The α(λ) curves of pure silicon and 1×10^{16} ions/cm^2 S-implanted silicon.

Table 1, below: Refractive index and absorption coefficient at α = 700 nm.

Implanted Element	Implantation Dose (ions/cm^2)	Refractive Index	Absorption Coefficient (cm^{-1})	% Difference from Ordinary Si
Ordinary Si	—	3.769	1560	—
Sulfur	1×10^{15} ion/cm^2 ~ 0.08 at. %	3.045	1688	~ 8%
	1×10^{16} ion/cm^2 ~ 0.8 at. %	2.775	7440	~ 400%
Selenium	1×10^{14} ion/cm^2 ~ 0.008 at. %	3.017	2687	~ 70%
	1×10^{15} ion/cm^2 ~ 0.08 at. %	3.094	2814	~ 80%
	1×10^{16} ion/cm^2 ~ 0.8 at. %	2.969	9692	~ 500%
	3×10^{16} ion/cm^2 ~ 2.3 at. %	2.758	15775	~ 1000%
Tellurium	1×10^{16} ion/cm^2 ~ 0.8 at. %	3.17	7029	~ 400%
Phosphorous	1×10^{16} ion/cm^2 ~ 0.8 at. %	3.055	5088	~ 200%
Arsenic	1×10^{16} ion/cm^2 ~ 0.8 at. %	3.255	3440	~ 100%
Boron	1×10^{16} ion/cm^2 ~ 0.8 at. %	3.383	2583	~ 70%